Signal, Image and Video Processing (2022) 16:1297–1304
https://doi.org/10.1007/s11760-021-02081-3

ORIGINAL PAPER

Single-image dehazing using scene radiance constraint and color gradient guided filter

Haonan Han[1,2] · Feng Qian[1] · Bao Zhang[1]

Received: 26 July 2020 / Revised: 14 May 2021 / Accepted: 31 October 2021 / Published online: 20 January 2022

Abstract
Haze and other types of atmospheric particles limit visibility and reduce image contrast, which will seriously influence the visual system. In recent years, most existing single-image dehazing algorithms have made significant progress. However, most of the existing dehazing algorithms suffer from under- or over-enhancement, color distortion and halo artifacts. The dark channel prior which is widely recognized also has such problems due to improper assumptions or operations. To solve these problems, in this paper, a scene radiance constraint is proposed to remove haze and a color gradient guided filter is proposed to refine the initial transmission map. From the experimental results, it is demonstrated that the proposed method achieves excellent performance compared with the representative dehazing methods in terms of image's visibility and color restoration.

Keywords Dark channel prior · Scene radiance constraint · Color gradient guided filter

1 Introduction

Haze is universal weather in outdoor imaging. Images acquired with haze often have low contrast and poor visibility. In a hazy weather, due to the absorption and scattering of atmospheric particles, reflected light from an object will be directly attenuated, and the atmospheric light will also be scattered into the imaging system. Thus, the colors of the scene get faded and become more similar to the haze. The existence of haze dramatically affects the visual system and brings certain difficulties to target tracking and recognition.

Although single-image dehazing is a challenging ill-posed problem, many assumptions and priors have made significant progress [1–10]. Color attenuation prior (CAP) [1] states that the difference between the brightness and the saturation is highly related to the concentration of haze in the hazy image. The difference between the brightness and the saturation can be utilized to dehaze. Multi-scale convolutional neural networks dehazing (MSCNN) [4] and DehazeNet [5] are learning-based methods which use the dataset to learn effective features and the trained model can be utilized to dehaze. Non-local dehazing (NLD) [3,11] state that colors of the haze-free image are clustered in RGB space. The pixels become haze-lines passing through the atmospheric light under the influence of haze. The distance between pixel and atmospheric light in a hazy-line is highly correlated with the concentration of haze. Dark channel prior (DCP) [2] is the most popular dehazing algorithm and various dehazing algorithms have been proposed to improve it.

Dark channel prior is a fast and reliable single-image dehazing algorithm. The prior can achieve a quite compelling dehazing results. However, the prior is not always accurate, when some objects in the scene are brighter than atmospheric light, dark channel prior will fail and cannot correctly estimate initial transmission map. Besides, the estimation of initial transmission map always suffers from block artifacts and noise. The transmission map should be refined. However edge-preserving smoothing techniques such as the guided image filter (GIF) [12] and weighted guided image filter (WGIF) [13] always over smooth images and produce halo artifacts. In this paper, scene radiance constraint and

✉ Haonan Han
hanhaonan16@mails.ucas.edu.cn

Feng Qian
tsienfung@126.com

Bao Zhang
zhangb@ciomp.ac.cn

[1] Changchun Institute of Optics, Fine Mechanics and Physics, Chinese Academy of Sciences, Changchun 130033, China

[2] University of Chinese Academy of Sciences, Beijing 100049, China

color gradient guided filter are introduced to address these problems.

Other sections of the paper are arranged as follows: The dark channel prior is briefly reviewed in Sect. 2. Section 3 presents the proposed method in detail. Experimental results are presented in Sect. 4 to verify the dehazing effect. The paper is finally summarized in Sect. 5.

2 Previous work

The atmospheric scattering model [15–17] with hazy images is widely denoted by:

$$I(x) = J(x)t(x) - A(1 - t(x)) \tag{1}$$

where x denotes the pixel coordinates, $I(x)$ is the observed image with haze, and $J(x)$ is the corresponding image without haze, $t(x)$ is the transmission, A is the atmospheric light.

Dark channel prior [2] was found after extensive observation on haze-free images (except for sky areas and white areas): in most local blocks, there is a color channel with very low intensity values close to zero. Minimizing all pixels in the block to calculate the dark channel:

$$J^{\text{dark}}(x) = \min_{c\in r,g,b}\left(\min_{y\in\Omega(x)} J^c(y)\right) \tag{2}$$

where Ω represents a window of squares with x as the center pixel, J^c is a certain RGB color channel of J. Atmospheric light A is estimated as the brightest pixel in the hazy image corresponding to 0.1% of the highest intensity in dark channel. It is assumed that the transmission of each local block $\Omega(x)$ is constant. In this paper, the block's transmission is presented by $\tilde{t}(x)$. The minimization operation for the atmospheric scattering model (1) in the local block is calculated:

$$\min_{y\in\Omega(x)}(I^c(y)) = \tilde{t}(x)\min_{y\in\Omega(x)}(J^c(y)) + (1 - \tilde{t}(x))A^c \tag{3}$$

Further, by taking the minimum operation on the above equation among three color channels, the following is obtained:

$$\min_c\left(\min_{y\in\Omega(x)}\left(\frac{I^c(y)}{A^c}\right)\right) = \tilde{t}(x)\min_c\left(\min_{y\in\Omega(x)}\frac{J^c(y)}{A^c}\right) + (1 - \tilde{t}(x)) \tag{4}$$

It is known that the $J^{\text{dark}}(x)$ of the haze-free image J approaches 0. The transmission $\tilde{t}(x)$ is estimated:

$$\tilde{t}(x) = 1 - \min_c\left(\min_{y\in\Omega(x)}\left(\frac{I^c(y)}{A^c}\right)\right). \tag{5}$$

The haze concentration and dark channel are highly correlated in the hazy image. The prior can achieve a quite satisfactory dehazing results. However, the prior is not always accurate. According to Eq. 5, dark channel prior will fail if some objects in the scene are brighter than the atmospheric light.

$$\min_c\left(\min_{y\in\Omega(x)}\left(\frac{I^c(y)}{A^c}\right)\right) \geq 1, \quad \text{and} \quad \tilde{t}(x) \leq 0. \tag{6}$$

Besides, when smoothing the initial transmission map with the original guided filter [12], it is not ideal for halo artifacts suppression. For its constant regularization parameter has excessive smoothing effect around the edges which may produce halo artifacts.

In the next section, a transmission estimation method using the scene radiance constraint is proposed to address the shortcoming of dark channel prior. We also introduce color gradient guided filter to reduce halo artifacts.

3 Proposed method

3.1 Scene radiance constraint

Dark channel prior [2] has the above-mentioned problems due to its incomplete assumption. In other words, dark channel prior needs further research and development. Equation (1) is transformed as:

$$J(x) = \frac{1}{t(x)}(I(x) - A) + A. \tag{7}$$

In order to acquire the dehazed image $J(x)$, transmission $t(x)$ and atmospheric light A need to be estimated. Atmospheric light A is generally determined by picking particular pixels of hazy images or using some specific methods. Atmospheric light A is estimated in this paper through dark channel prior, due to its simplicity and efficiency. Next, the initial transmission map $t(x)$ is obtained by using inherent scene radiance constraint.

The scene radiance has an inherent constraint which can be written as:

$$0 \leq J_c(x) \leq 255. \tag{8}$$

The constraints on $t(x)$ are derived from Eqs. (7) and (8):

$$t(x) \geq \frac{I_c(x) - A_c}{-A_c} \tag{9}$$

$$t(x) \geq \frac{I_c(x) - A_c}{255 - A_c}. \tag{10}$$

The two constraints can be combined into a lower bound $t_{\mathrm{lb}}(x)$:

$$t_{\mathrm{lb}}(x) = \max\left\{\max_{c\in r,g,b}\left\{\frac{I_c(x)-A_c}{-A_c}\right\}, \max_{c\in r,g,b}\left\{\frac{I_c(x)-A_c}{255-A_c}\right\}\right\} \tag{11}$$

$$0 \le t_{\mathrm{lb}}(x) \le t(x) \le 1. \tag{12}$$

We establish a cost function that includes smoothness term and boundary term and estimate the initial transmission map by minimizing this cost function.

$$E(t) = \sum_x \sum_{y\in N(x)} \frac{|t(x)-t(y)|}{||I(x)-I(y)||_2^2} + \sum_x B(x) \tag{13}$$

where $y \in N(x)$ indicates y is a neighboring pixel of x.

The smoothness term is constructed by assuming that neighboring pixels with similar colors share similar transmissions. The boundary term is constructed based on lower bound constraint and dark channel prior [2]. For dark channel prior, pixels of a local block $\Omega(x)$ have at least one dark pixel. But it is impossible to verify which pixels in hazy image are dark pixels, because pixels that do not satisfy $\min_c I^c(x) = 0$ can always be explained as dark pixels affected by haze. For this problem, we consider every pixel that satisfies the lower bound constraint as a potentially dark pixel to preserve all possibilities [18]. Therefore, it is further assumed that the lower bound of all pixels in the local block $\Omega(x)$ are candidates of $t(x)$. The label set $L(x)$ is defined by the lower bound constraint and the dark channel prior as:

$$L(x) = \{t_{\mathrm{lb}}(y) | t_{\mathrm{lb}}(y) > t_{\mathrm{lb}}(x),\, y \in \Omega(x)\}. \tag{14}$$

The boundary term is obtained from the label set

$$B(x) = \begin{cases} 0 & t(x) \in L(x) \\ \infty & t(x) \notin L(x) \end{cases}. \tag{15}$$

It is worthy to point out that if we replace the preserving all possibilities with the local constant assumption, the label set becomes $L(x) = \max_{y\in\Omega(x)} t_{\mathrm{lb}}(y)$, where the first constraint is the same as that of the dark channel prior. In addition, when some objects in the scene are brighter than atmospheric light, dark channel prior cannot correctly estimate the transmission. Therefore, the proposed algorithm uses an additional constraint that is used to prevent the overflow of recovered pixel values.

The typical multi-label problem of minimizing the cost function is solved by α-expansion [19–21]. α-expansion makes the cost function decrease by adjusting one label per expansion, traversing all labels until the cost function fails to decrease in all expansions of the adjusted labels, and the algorithm stops and reaches a local optimum, which results in an optimal solution for the initial transmission map. The initial transmission map that introduces redundant edges and noise should be corrected. However, edge-preserving smoothing techniques will always over smooth images and thus produce halo artifacts. Fortunately, these artifacts can be attenuated by the proposed color gradient guided filter.

3.2 Color gradient guided filter

For the original guided filter [12], the fixed regularization parameter λ has the same smoothness. When considering image smoothing and edge-preserving together, edge smoothing may be unavoidable due to the constant regularization parameter λ. In other words, halo artifacts are unavoidable for the original guided filter in some cases. To attenuate the halo artifacts, we design the color gradient guided filter by introducing the weight φ to guided filter. The critical precondition for guided filter is the local linear model which ensures that the filtered image q_i has edges only when the guidance image I has edges. It needs to be solved by maintaining the local linear model while minimizing the difference between the initial transmission map $t(x)$ and refined transmission map $\tilde{t}(x)$:

$$E = \sum_{x\in\omega_k}\left((a_k I(x) + b_k - t(x))^2 + \frac{\lambda}{\varphi(x)}a_k^2\right) \tag{16}$$

where ω_k represents a square window with a pixel k centered, a_k and b_k are two constants, φ is the adaptive edge aware weight. Compared with original guided filter, we introduce an adaptive weight [13,14] so that the constant regularization parameter can adjust adaptively according to different cases. The ideal weight model requires that pixels have a high weight at the edge and a low weight at the non-edge. Therefore, the gradient information of pixels can be amplified or suppressed by designing a weight based on the exponential function. φ is defined as follows:

$$\varphi(x) = \begin{cases} \epsilon + \left(\frac{\mathrm{CG}(x)}{k}\right)^{\frac{\mathrm{CG}(x)}{k}} & \mathrm{CG}(x) \ge k \\ \epsilon + \frac{1}{\left(\frac{k}{\mathrm{CG}(x)}\right)^{\frac{k}{\mathrm{CG}(x)}}} & \mathrm{CG}(x) < k \end{cases} \tag{17}$$

where $\mathrm{CG}(x)$ [22] is the color gradient map of the guidance image I, k is the threshold used to determine edges, and its value is chosen as $\mathrm{mean}(\mathrm{CG}(x))$, ϵ is a constant chosen to be $(0.001 \times \mathrm{DR})^2$, DR is the dynamic scope of image to be filtered.

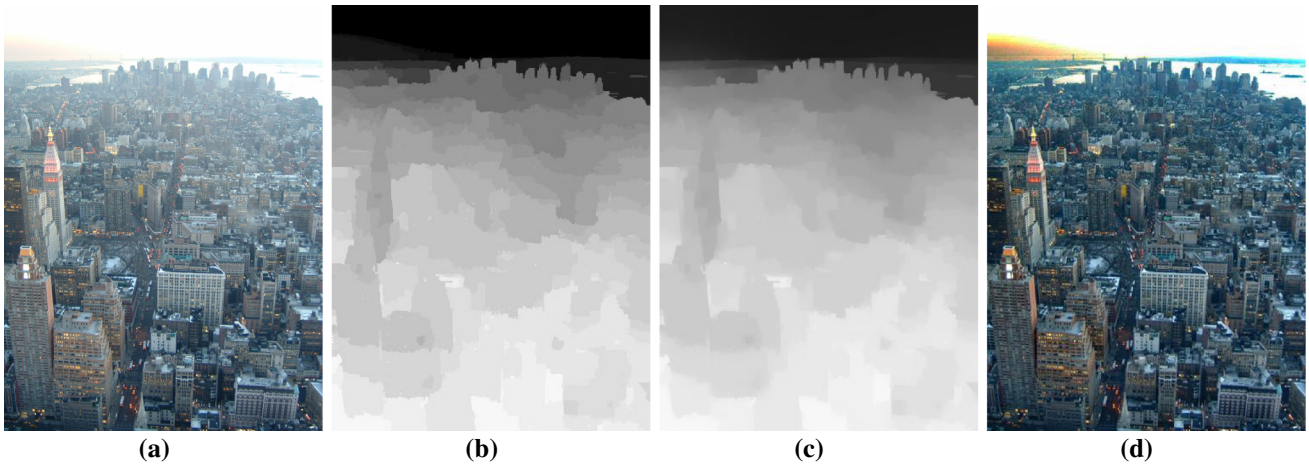

Fig. 1 Dehazing result. **a** Hazy image; **b** Initial transmission map; **c** Refined transmission map by the proposed CG-GIF; **d** Dehazed image

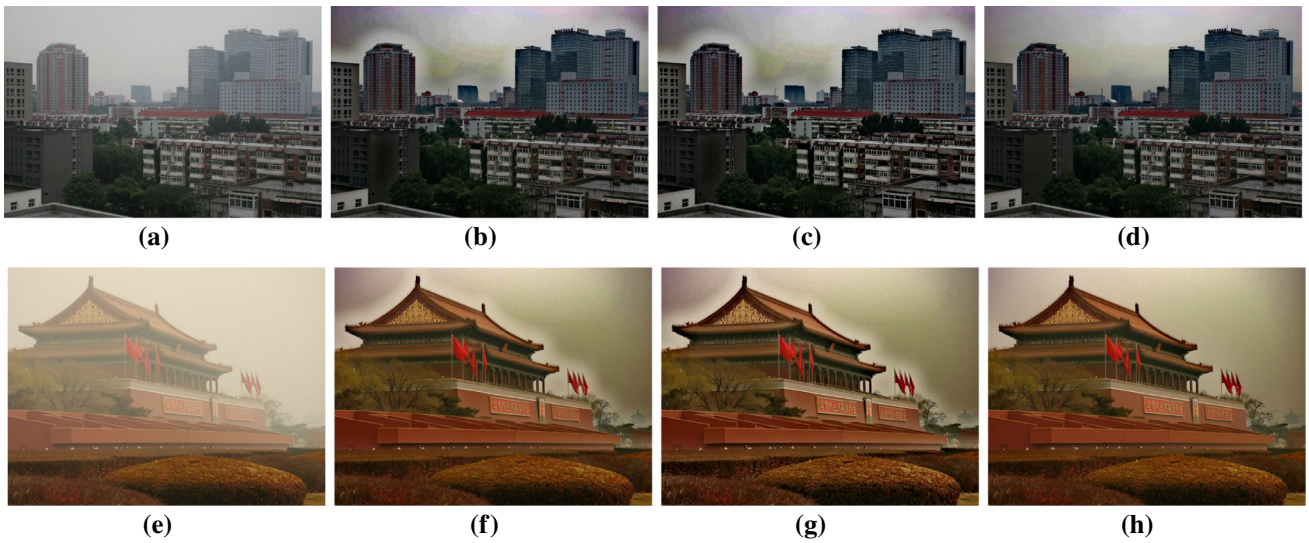

Fig. 2 Comparison of the GIF, the WGIF and Ours. **a**, **e** Hazy images; **b**, **f** Dehazed results by the GIF; **c**, **g** Dehazed results by the WGIF; **d**, **h** Dehazed results by ours. Both GIF and WGIF suffer from halo artifacts while our proposed CG-GIF effectively suppresses halo artifacts

The optimal solutions of a_k and b_k are calculated as:

$$a_k = \frac{\frac{1}{|\omega|}\sum_{x\in\omega_k} I(x)t(x) - \mu_k \bar{t}(x)}{\sigma_k^2 + \frac{\lambda}{\varphi(x)}} \tag{18}$$

$$b_k = \bar{t}(x) - a_k \mu_k \tag{19}$$

where μ_k is the mean of I, and σ_k^2 is the variance of I, $|\omega|$ is the number of pixels, and $\bar{t}(x) = \frac{1}{|\omega|}\sum_{x\in\omega_k} t(x)$ is the mean of $t(x)$. After obtaining the linear coefficients (a_k, b_k), the refined transmission map $\tilde{t}$ is calculated by the following equation:

$$\tilde{t}(x) = \bar{a}(x)I(x) + \bar{b}(x) \tag{20}$$

where $\bar{a}(x)$ and $\bar{b}(x)$ are the averages of a_k and b_k for all windows, calculated as:

$$\bar{a}(x) = \frac{1}{|\omega_x|}\sum_{k\in\omega_x} a_k \tag{21}$$

$$\bar{b}(x) = \frac{1}{|\omega_x|}\sum_{k\in\omega_x} b_k, \tag{22}$$

where $|\omega_x|$ is the cardinality of ω_x.

Figure 1c is the result of refined transmission map. Due to the regularization step, noise in the initial transmission map is suppressed, edges and outlines of objects can be found. The dehazed image $J(x)$ is derived by:

$$J(x) = \frac{I(x) - A}{\max(\tilde{t}(x), t_0)} + A \tag{23}$$

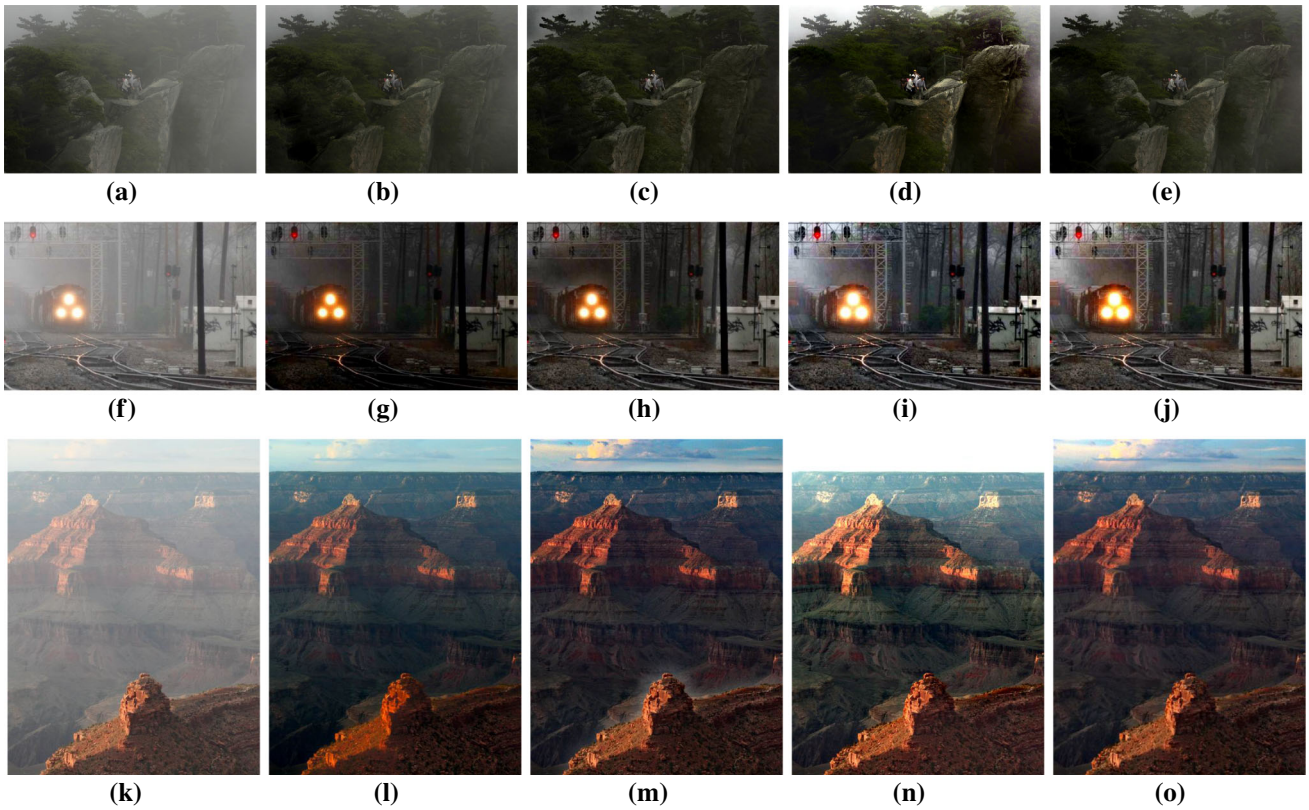

Fig. 3 Comparison of the proposed dehazing algorithm and the dehazing algorithms in CAP, DCP, NLD via hazy images. **a**, **f**, **k** Hazy images; **b**, **g**, **l** Dehazed results by CAP; **c**, **h**, **m** Dehazed results by DCP; **d**, **i**, **n** Dehazed results by NLD; **e**, **j**, **o** Dehazed results by proposed method

where the value of t_0 is set to 0.1. To avoid noise amplification, a lower limit t_0 is restricted on the transmission map $\tilde{t}(x)$.

4 Experiment

4.1 Qualitative results

The proposed CG-GIF is used to compare with GIF [12] and WGIF [13] for single-image haze removal. To be fair, we use the same haze removal method for both GIF and WGIF. As shown in Fig. 2, both GIF and WGIF can over smooth images and produce halo artifacts, especially in the fine structure regions. Clearly, the proposed CG-GIF can effectively suppress halo artifacts and preserve the edges of objects.

The proposed dehazing method is in comparison with three other representative dehazing methods [1–3] by six hazy images. All parameters are set according to the parameters picked by the algorithms in [1–3]. In Figs. 3 and 4, the algorithm in [1] works well for haze removal in the thin haze, but it does not work well when the haze is thick. The reason for this is that the scattering coefficient and the learned linear model coefficients are fixed. These coefficients need to be adaptively adjusted according to the concentration of haze in hazy image. It is demonstrated in Figs. 3 and 4 that the algorithm in [2] dehazes well but the transmission map of [2] has redundant details which are not related to the amount of haze. As a result, the contrast of the dehazed images is underestimated. Moreover, the dehazed images produce halo artifacts in edge areas. It is confirmed in Figs. 3 and 4 that the algorithm in [3] can perform better haze removal than other dehazing algorithms but it may appear wrong clustering the pixels into haze-lines and lead to color shifts. Experimental comparison reveals that the proposed algorithm generates quite better dehazing results with faithful color and few halo artifacts.

4.2 Quantitative results

Good dehazing methods need to enhance image visibility and preserve image color and structure. To quantitatively evaluate these dehazing methods, we calculate the image visibility metric visual contrast measure (VCM) [23], the color restoration metric blind assessment indicator σ [24] and the structural similarity (SSIM) [25].

The visual contrast measure (VCM) is an objective evaluation method that can evaluate image visibility. VCM calculates the variance of each sub-area after dividing the image into several sub-areas and counts the proportion of the

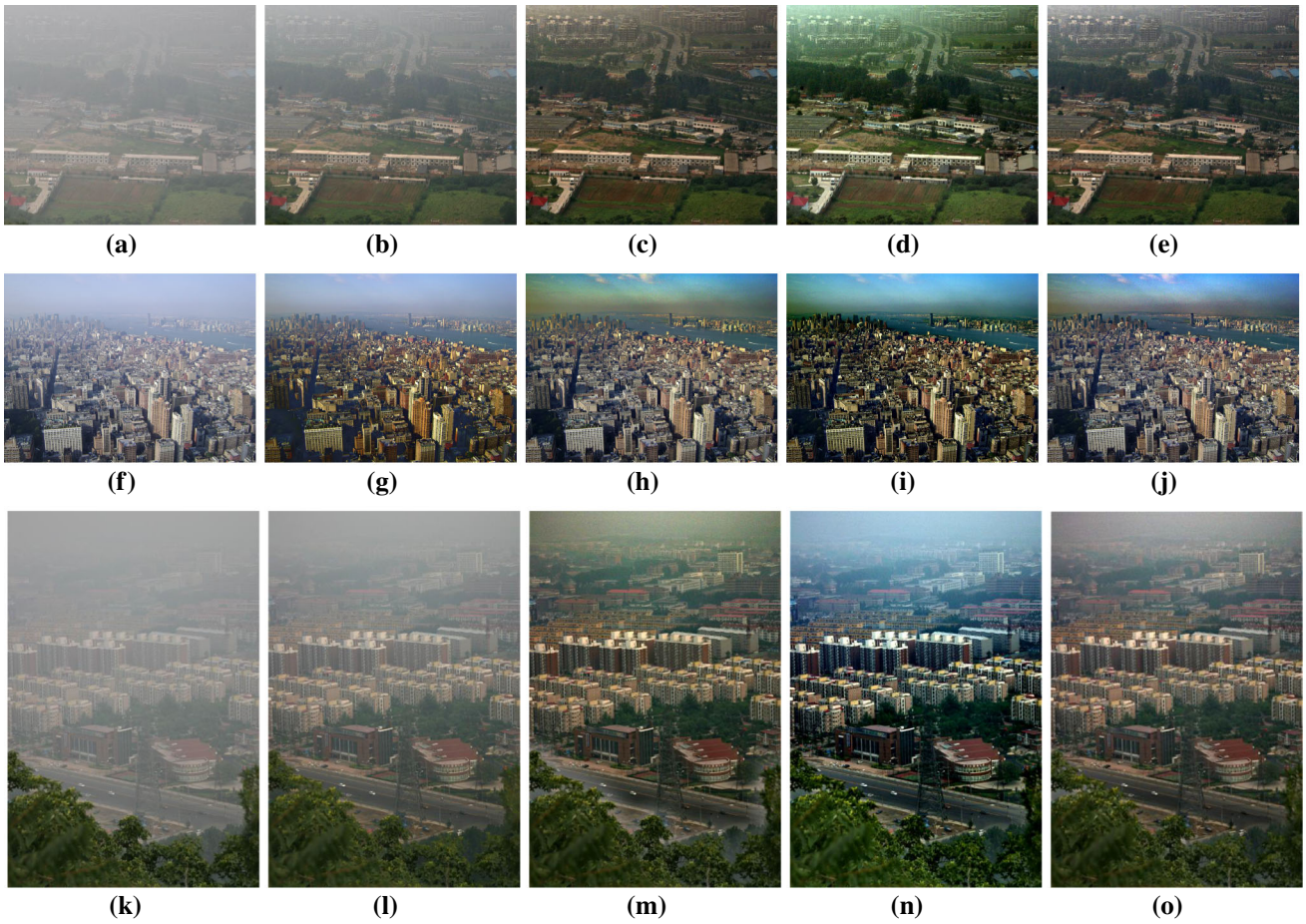

Fig. 4 Comparison of the proposed dehazing algorithm and the dehazing algorithms in CAP, DCP, NLD via hazy images. **a**, **f**, **k** Hazy images; **b**, **g**, **l** Dehazed results by CAP; **c**, **h**, **m** Dehazed results by DCP; **d**, **i**, **n** Dehazed results by NLD; **e**, **j**, **o** Dehazed results by proposed method

number of sub-areas with variance higher than the threshold to the number of all areas, which is defined as:

$$\mathrm{VCM} = 100 * A_v / A_t, \tag{24}$$

where A_v denotes the number of sub-areas whose is exceeds the threshold, A_t denotes the number of all sub-areas in a single image. In our experiments, the OTSU threshold image segmentation algorithm is chosen to calculate the threshold adaptively. The better the visibility of the dehazed image, the higher the VCM.

The blind assessment indicator σ [24] is an objective evaluation method that can evaluate color restoration of dehazed images. Hazy images are affected by haze and color saturation is decreased, so σ is calculated as the ratio of saturated pixels after image dehazing:

$$\sigma = \frac{n_s}{M * N}, \tag{25}$$

where M and N indicate the image width and height and n_s indicates the number of saturated pixels of dehazed image. The better the color restoration, the smaller the σ.

Structural similarity (SSIM) [25] is an objective evaluation method that can evaluate the structural similarity ability between hazy image $I(x)$ and dehazed image $J(x)$, and it is calculated as:

$$\mathrm{SSIM}(I, J) = [l(I, J)]^{\alpha} \cdot [c(I, J)]^{\beta} \cdot [s(I, J)]^{\gamma}, \tag{26}$$

where l, c, s are luminance, contrast and structure comparison function, respectively. α, β and γ are weights to adjust the three comparison function. l, c and s are calculated as

$$l(I, J) = \frac{2\mu_I \mu_J + C_1}{\mu_I^2 + \mu_J^2 + C_1} \tag{27}$$

$$c(I, J) = \frac{2\sigma_I \sigma_J + C_2}{\sigma_I^2 + \sigma_J^2 + C_2} \tag{28}$$

$$s(I, J) = \frac{\sigma_{IJ} + C_3}{\sigma_I \sigma_J + C_3} \tag{29}$$

Table 1 Quantitative comparison

Algorithms	VCM	σ	SSIM	t
CAP	68.2692	0.0004	0.8666	**0.9089**
DCP	73.4615	0.0006	0.8661	1.0259
NLD	77.1154	0.0054	0.6834	9.5947
Ours	**78.1538**	**0.0001**	**0.8706**	1.2337

Bold values indicate the best performance

Table 2 Quantitative comparison

Algorithms	VCM	σ	SSIM	t
CAP	24.5000	0.0081	0.8107	**0.6519**
DCP	40.1667	0.0019	0.5994	0.7921
NLD	27.1667	0.0037	0.5419	7.6626
Ours	**41.6667**	**0.0005**	**0.8359**	0.9449

Bold values indicate the best performance

where μ_I is the mean of I, μ_J is the mean of J, σ_I^2 is the variance of I, σ_J^2 is the variance of J, σ_{IJ} is the covariance of I and J. The constant C_1, C_2 and C_3 are included to avoid instability. A higher SSIM indicates that the hazy and dehazed images are more similar in terms of structure.

The results listed in Tables 1 and 2 demonstrate that the proposed method performs best on all metrics. The comparisons show that the proposed method can recover haze-free images with faithful color and high image visibility. However, the computation cost of the proposed algorithm is slightly higher than original dark channel prior.

5 Conclusion

In this paper, a haze removal algorithm based on the dark channel prior and the inherent scene radiance constraint is proposed. When some objects in the scene are brighter than the atmospheric light, the inherent scene radiance constraint is still valid. For each pixel, we build a label set that preserves all possibilities in place of the local constant assumption. The label set fully exploits dark channel prior. Therefore, the proposed method can estimate the transmission map more reliably. Besides, we propose a color gradient guided filter by introducing a weight φ to GIF. Processing images with the proposed filter is able to preserve better details than existing guided filters in regions of the structure and effectively suppresses the generation of halo artifacts. Our method can be visually quite satisfying results in a cost of moderate computational cost increasement.

References

1. Zhu, Q., Mai, J., Shao, L.: A fast single image haze removal algorithm using color attenuation prior. IEEE Trans. Image Process. **24**(11), 3522–3533 (2015)
2. Kaiming, H., Jian, S., Xiaoou, T.: Single image haze removal using dark channel prior. In: IEEE Conference on Computer Vision and Pattern Recognition, pp. 1956–1963 (2009)
3. Berman, D., Treibitz, T., Avidan, S.: Non-local image dehazing. In: IEEE Conference on Computer Vision and Pattern Recognition, pp. 1674–1682 (2016)
4. Ren, W., Liu, S., Zhang, H., Pan, J., Cao, X., Yang, M.-H.: Single image dehazing via multi-scale convolutional neural networks. In: European Conference on Computer Vision ECCV 2016, Cham, pp. 154–169 (2016)
5. Cai, B., Xu, X., Jia, K., Qing, C., Tao, D.: DehazeNet: an end-to-end system for single image haze removal. IEEE Trans. Image Process. **25**(11), 5187–5198 (2016)
6. Sulami, M., et al.: Automatic recovery of the atmospheric light in hazy images. In: IEEE International Conference on Computational Photography (2014)
7. Meng, G., et al.: Efficient image dehazing with boundary constraint and contextual regularization. In: IEEE International Conference on Computer Vision (2013)
8. Tan, R.T.: Visibility in bad weather from a single image. In: IEEE Conference on Computer Vision and Pattern Recognition (2008)
9. Fattal, R.: Single image dehazing. ACM Trans. Graph. **27**(3), 72 (2008)
10. Fattal, R.: Dehazing using color-lines. ACM Trans. Graph. **34**(1), 13:1-13:14 (2014)
11. Berman, D., Treibitz, T., Avidan, S.: Air-light estimation using haze-lines. In: IEEE International Conference on Computational Photography, pp. 1–9 (2017)
12. He, K., Sun, J., Tang, X.: Guided image filtering. IEEE Trans. Pattern Anal. Mach. Intell. **35**(6), 1397–1409 (2013)
13. Li, Z., Zheng, J., Zhu, Z., Yao, W., Wu, S.: Weighted guided image filtering. IEEE Trans. Image Process. **24**(1), 120–129 (2015)
14. Kou, F., Chen, W., Wen, C., Li, Z.: Gradient domain guided image filtering. IEEE Trans. Image Process. **24**(11), 4528–4539 (2015)
15. Hide, R.: Optics of the atmosphere: scattering by molecules and particles. Phys. Bull. **28**(11), 521 (1977)
16. Narasimhan, S.G., Nayar, S.K.: Contrast restoration of weather degraded images. IEEE Trans. Pattern Anal. Mach. Intell. **25**(6), 713–724 (2003)
17. Nayar, S.K., Narasimhan, S.G.: Vision in bad weather. In: Proceedings of the Seventh IEEE International Conference on Computer Vision, vol. 2, pp. 820–827 (1999)
18. Zhu, M., He, B., Wu, Q.: Single image dehazing based on dark channel prior and energy minimization. IEEE Signal Process. Lett. **25**(2), 174–178 (2018)
19. Boykov, Y., Veksler, O., Zabih, R.: Fast approximate energy minimization via graph cuts. IEEE Trans. Pattern Anal. Mach. Intell. **23**(11), 1222–1239 (2001)
20. Kolmogorov, V., Zabin, R.: What energy functions can be minimized via graph cuts? IEEE Trans. Pattern Anal. Mach. Intell. **26**(2), 147–159 (2004)
21. Boykov, Y., Kolmogorov, V.: An experimental comparison of min-cut/max-flow algorithms for energy minimization in vision. IEEE Trans. Pattern Anal. Mach. Intell. **26**(9), 1124–1137 (2004)
22. Gonzalez, R. C., Woods, R. E., Eddins, S. L.: Digital Image Processing Using Matlab, pp. 149–152. Publishing House of Electronics Industry, Beijing (2004)

23. Jobson, D.J., Rahman, Z.U., et al.: A comparison of visual statistics for the image enhancement of FORESITE aerial images with those of major image classes. In: Proceedings of SPIE—The International Society for Optical Engineering (2006)
24. Hautiere, N., Tarel, J.P., et al.: Blind contrast enhancement assessment by gradient ratioing at visible edges. Image Anal. Stereol. **27**(2), 87–95 (2011)
25. Wang, Z., Bovik, A.C., et al.: Image quality assessment: from error visibility to structural similarity. IEEE Trans. Image Process. **13**, 600–612 (2004)